actuators

MDPI

Article

Displaying Tactile Sensation by SMA-Driven Vibration and Controlled Temperature for Cutaneous Sensation Assessment

Tomohiro Nozawa [1,*], Renke Liu [1] and Hideyuki Sawada [2]

[1] Department of Pure and Applied Physics, Waseda University, Tokyo 169-8555, Japan; askar_liu@fuji.waseda.jp
[2] Faculty of Science and Engineering, Waseda University, Tokyo 169-8555, Japan; sawada@waseda.jp
* Correspondence: nzw_3421@fuji.waseda.jp

Abstract: In this paper, we propose a novel tactile display that can present vibration patterns and thermal stimuli simultaneously. The vibration actuator employs a shape memory alloy (SMA) wire to generate micro-vibration with a frequency control of up to 300 Hz. The micro-vibration is conducted to a tactile pin for amplifying the vibration, to be sufficiently recognized by a user. A thermal stimulation unit, on the other hand, consists of four Peltier elements with heatsinks for heat radiation. Four vibration actuators and a thermal unit are arranged in a flat plane with a size of 20 mm × 20 mm, on which a user places the tip of an index finger to feel the presented vibratory stimuli under different temperature conditions. We conducted an experiment by employing nine subjects to evaluate the performance of the proposed tactile display and also to investigate the effects of temperature on recognizing tactile sensation. The results demonstrated that the proposed device was feasible for the quantitative diagnosis of tactile sensation. In addition, we verified that the sensitivity of tactile sensation decreased with colder stimuli.

Keywords: tactile display; shape memory alloy; vibration; temperature

check for updates

Citation: Nozawa, T.; Liu, R.; Sawada, H. Displaying Tactile Sensation by SMA-Driven Vibration and Controlled Temperature for Cutaneous Sensation Assessment. *Actuators* **2024**, *13*, 463. https://doi.org/10.3390/act13110463

Academic Editors: Wei Min Huang, Hongli Ji, Todor Stoilov Todorov and Rosen Mitrev

Received: 25 September 2024
Revised: 30 October 2024
Accepted: 16 November 2024
Published: 18 November 2024

1. Introduction

Tactile interaction devices that artificially stimulate the human skin are rapidly growing thanks to recent technological advancements [1]. So far, various tactile displays have been proposed mainly to enhance immersion into virtual reality (VR) and augmented reality (AR) systems. For instance, tactile displays for interaction with balls [2] and presenting textures [3] and edge inclination [4] of virtual objects have been introduced. In addition to the applications for VR/AR systems, tactile displays can also be applied in evaluations of human tactile sensations [5,6] and assistance for visually impaired people [7–9].

In the medical field, some anti-cancer drugs exert neurotoxic effects, which result in distortions of thermal sensation, nerve damage, and so on [10]. Moreover, tumor-bearing patients suffer from several symptoms, including cold sensations [11]. Therefore, the knowledge of distorted tactile sensation, thermal effects on sensitivity, and their interaction are also important in medical development.

Mechanoreceptors and thermoreceptors are distributed throughout the skin, playing roles in perceiving external stimuli. Recently, multisensory temperature and vibration display devices have attracted attention, and several challenges, such as large power consumption and limited variation of stimulations, remain in this research field.

In this study, to address these challenges, we employ shape memory alloy (SMA) wire-based vibration actuators and Peltier elements for temperature control. SMAs are notable materials that exhibit unique physical properties [12] and have been applied in various ways, such as tactile feedback [13,14], transducers [15], vibrators [16], tendons of robotic fingers [17], and actuators of soft robots [18]. SMA wire-based actuators enabled us to achieve a tactile feedback system that can be driven with low voltage and controlled independently and quantitively.

This paper proposes a novel tactile display for the simultaneous presentation of vibratory and temperature stimuli to diagnose tactile sensation. The development of a tactile display that can control vibration and thermal stimulus quantitively with easy operations will be described, together with the performance evaluation of the device through a user experiment. The results also provide data on sensitivity under different temperature conditions, which will be effectively employed in the medical field.

The article is organized as follows. Firstly, the related works are described in Section 2. Section 3 presents the hardware and software design of the novel tactile display. The parameter selection and determination for tactile assessments are described in Section 4, and then a user experiment is presented in Section 5. In Section 6, the experimental results are discussed, and the study is summarized in the conclusion chapter.

2. Related Works

Human skin is an excellent medium for perceiving and interacting with the surrounding environment [19]. It covers the entire body and enables perceptions of external stimuli like touching [20].

Human skin has four types of mechanical receptor units: RA I (Rapidly Adapting type one), RA II (Rapidly Adapting type two), SA I (Slowly Adapting type one), and SA II (Slowly Adapting type two) [21]. Each unit responds differently to the motion and deformation of the skin [22]. By perceiving the properties of objects with these receptors, we can grasp them with proper force [23]. Among the four types of units, RA I and RA II present high sensitivity between 5–50 Hz and 30–500 Hz, respectively [24], with the lowest thresholds at approximately 20–40 Hz and 200–250 Hz, respectively [25].

In addition to the four mechanical receptor units, there are thermal receptors in the skin, and it is known that vibration and temperature interact with each other. Green et al. observed that for vibration with a frequency between 150 and 250 Hz, the perception threshold became greater when the skin was cooled and concluded that the sensitivity of RA II decreased by cooling [26]. Zhang et al. reported that raising the skin's temperature enhanced the ability to perceive vibration stimuli [27].

In recent years, multisensory vibration and temperature display devices have been developed. Yang et al. proposed a device composed of Peltier elements and a pin array of piezoelectric morphs [28]. The pins with a diameter of 0.7 mm were arranged in a 5×6 array with a spatial interval of 1.8 mm. The maximum deformation was over 700 μm, requiring a large voltage of 150 V. Singhal et al. built a device comprising a vibration motor and an annular Peltier device [29]. The maximum amplitude of the motor reached 1.48 m/s^2, with a frequency of 100 Hz. However, the number of the motor was only one, which made it challenging to form several vibration patterns compared to array-type vibration actuators. Singhal et al. achieved non-contact thermo-tactile feedback using an ultrasound display and ceramic heating elements [30]. Mid-air haptic, non-invasive feedback was realized, but the heating elements required a relatively long time to achieve the target temperature. Gallo et al. developed a multimodal tactile display using a Peltier element and a hybrid pneumatic and electromagnetic actuation [31]. The tactile cells were formed in a 2×2 array, with a spatial interval of 12 mm. Their patterns could be preserved without energy consumption but not driven at high frequencies due to their relatively long response time. Gharat et al. realized a haptic display consisting of eccentric rotating mass vibration motors and Peltier units [32]. The motors and Peltier units were arranged in 3×3 arrays, respectively. However, existing actuators are relatively large, making it hard to present multisensory stimulation to narrow regions of fingertips.

In the medical field, some instruments for tactile sensation evaluation have been proposed so far. For instance, measurements of pressure pain sensitivity were conducted using armature and coils [33]. In addition, the effect of texture shape on tactile sensation was investigated with plastic molds [34], and the gradual tactile sensory deficit was diagnosed by gratings [35]. In the diagnosis, some tools such as needles and test tubes have been used

for inspection; however, there are several challenges to shortening the inspection time and the quantitative diagnosis using numerical scores [33].

In this study, we developed a novel multimodal display using SMA-driven vibration actuators and a Peltier elements-based thermal stimulator. This device is driven by a single power supply with 5 V. Various vibration patterns are presented because each actuator can be driven independently with a wide frequency range and different intensity. These patterns can be easily adjusted by controlling the driving parameters. This device is also able to present thermal stimuli, both heating and cooling. In addition, the quantitative assessment of sensations is executed by employing the proposed device.

3. Novel Tactile Display Presenting Vibratory Stimuli and Controlled Temperature

We introduce the tactile display by combining SMA-based vibration actuators and a thermal stimulation unit for temperature presentation. Here, we describe the working principles, the structures, and the control methods of the actuators employed in the novel tactile display. Then, the assembling process to construct the whole system is presented.

3.1. SMA Actuator for Vibration Generation

In this work, we utilized SMA wires to provide precisely controlled vibrations. SMAs can be activated at low voltage, around 3 to 5 volts, with less energy consumption, allowing the thermal stimulation unit to be driven simultaneously with a single power supply. SMAs also enable us to fabricate vibration actuators with simple structures.

An SMA has two unique physical properties: shape memory effect and superelasticity. In this work, the former property was utilized for vibration presentation. The atomic structure at a lower temperature is called the Martensite phase, which is less symmetrical. On the other hand, the structure at a higher temperature is called the Austenite phase, which is highly symmetrical [36]. The structure transits between the two phases by the application or the removal of heat [37].

We employ Bio Metal Fiber 75 (Toki Corporation, Tokyo, Japan), with a length of 5 mm, to generate micro-vibrations. It is a filiform wire of NiTiCu-composite SMA that exhibits a one-way shape memory effect with a transition temperature of about 70 degrees Celsius. A filiform SMA wire shrinks up to 5% in the length direction when transformed to the Austenite phase from the Martensite phase (Figure 1). We fabricated the actuators, as shown in Figure 2a, using an SMA wire and a metal pin. The diameter of the pin is 0.76 mm, and a tiny hole is made at one end of the pin, through which the wire is passed so that the wire and the pin make contact with each other. Both ends of the wire are pinched using a copper plate, which is soldered on the circuit board to apply electric current for generating Joule's heat in the SMA body, resulting in an immediate temperature rise and wire shrinkage in the length direction. When the current stops, the heat in the body is immediately radiated, causing the wire to return to its original length in accordance with the temperature drop. By repeating the on–off of electric current, micro-vibration is generated in accordance with the wire deformation. The micro-vibration is effectively conducted to the metal pin to be mechanically amplified to large vibration, so that the user sufficiently perceives the vibratory stimuli by touching the other end of the pin, as shown in Figure 2b.

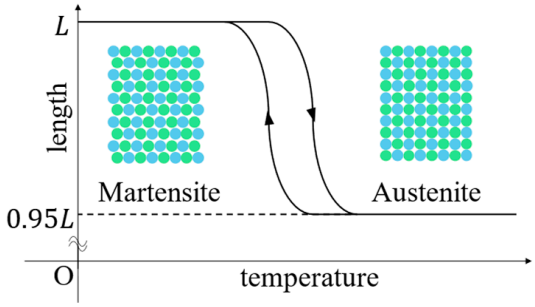

Figure 1. Illustration of shape memory effect.

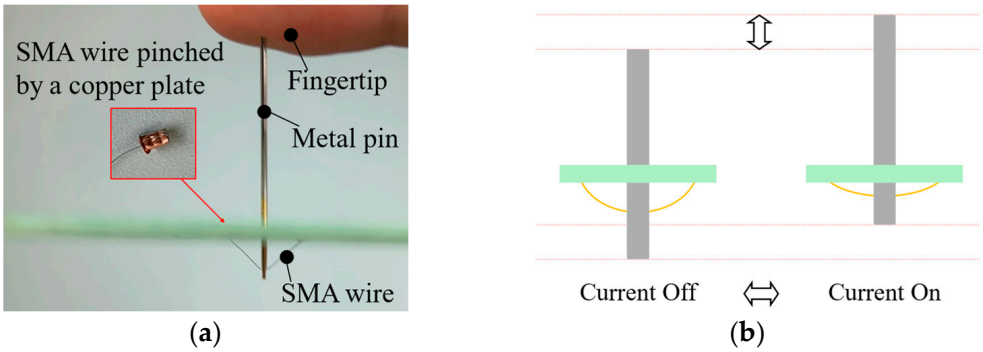

Figure 2. SMA actuator for vibration presentation: (**a**) Entire structure presenting stimuli to a fingertip; (**b**) Schematic illustration of the behavior.

The actuator is controlled by an electric current with pulse width modulation (PWM) using a Raspberry Pi microcomputer. Figure 3 shows an example of a pulse wave current. The pulses with W [s] width are given with L [s] time intervals. These values can be adjusted by controlling the frequency f [Hz] and the duty ratio d [%]. The width W and the time interval L are represented with the frequency f and the duty ratio d as $L = 1/f$ and $W = L \times (d/100) = d/100f$, respectively. The frequency means how many times pulses appear in a second, and we have confirmed that the actuator responds up to 300 Hz [38]. Vibrations with this frequency range are recognized as different tactile sensations by stimulating the RA I and/or RA II mechanoreceptors situated under the skin surface. The frequencies up to 50 Hz are recognized by the RA I receptors, and on the other hand, the frequencies greater than 30 Hz are perceived by the RA II receptors. The greater duty ratio supplies greater energy, which causes greater vibration as stronger vibratory stimuli. By controlling the frequencies and the duty ratios, the system is able to present various tactile stimuli to human tactile receptors.

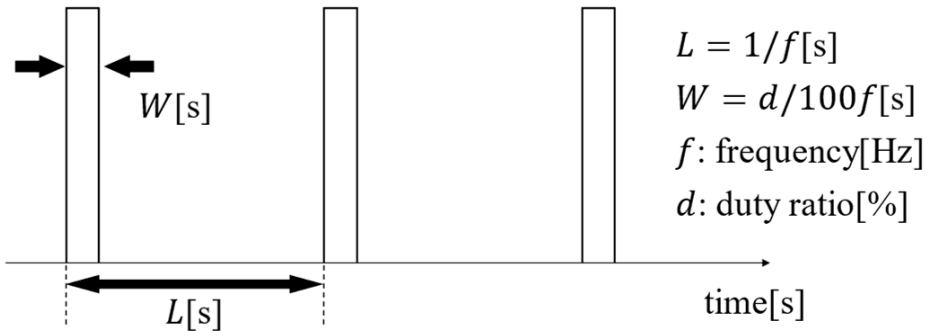

Figure 3. Pulse wave current.

3.2. Thermal Stimulation Unit for Temperature Control

A thermal stimulation unit based on the Peltier elements was fabricated to provide thermal stimuli from the display surface.

A Peltier element consists of P-type semiconductors and N-type semiconductors. When a direct current is provided to the junction of two types of semiconductors, heat transfer occurs according to the direction of the current, resulting in a temperature difference between the upper surface and the bottom one [39]. We employed TEC1-00703T125 (Kaito Denshi), which has a size of 10 mm × 10 mm. The thermal stimulation unit comprises four Peltier elements, four heatsinks, and a copper plate (Figure 4b,c). The heatsinks are settled in the bottom side of the display for heat radiation. The Peltier elements are arranged in a 2 × 2 array, and the copper plate is attached to the Peltier elements using conductive silicone. A thermistor (SEMITEC Corporation) is attached to the copper plate (Figure 4c) for measuring the temperature.

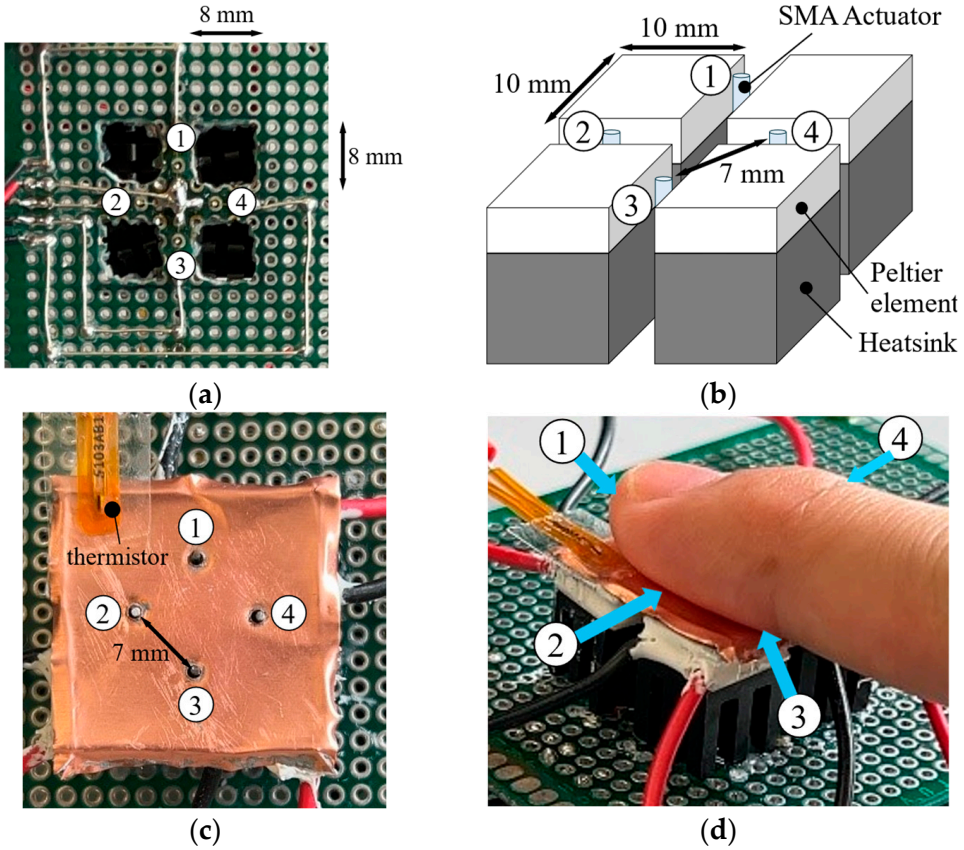

Figure 4. Structure of the tactile display: (**a**) Circuit board with four holes and the positions of SMA actuators; (**b**) Schematic illustration of the arrangement of actuators; (**c**) Top view of the tactile display with four SMA actuators covered by copper plate; (**d**) A finger placed on the display.

Like the SMA actuators, the thermal stimulation unit is also controlled by PWM. The duty ratio is controlled by a PID controller according to the surface temperature of the copper plate measured by the thermistor. The obtained temperature values are inputted into a Raspberry Pi in real time through an analog–digital converter. Large duty ratios increase the amount of heat transfer, resulting in a large change in temperature.

3.3. Design and Fabrication of the Tactile Display

The tactile display is fabricated by combining the SMA actuators and the thermal stimulation unit on a circuit board, as shown in Figure 4, which is integrated with a touch interface panel for user operations. First, as shown in Figure 4a, four holes with a size of 8 mm × 8 mm are cut out in the circuit board for effective heat dissipation. Four SMA wires are soldered at the four positions shown from 1 to 4. The distance between each SMA actuator is set at 7 mm, as shown in Figure 4b, which is approximately 3 times greater than the spatial resolution of the human fingertip as 2–3 mm [40], allowing users to discriminate the physical vibratory stimuli presented by the pins. Four Peltier elements on heatsinks are also placed on the 4 holes. The surface of the constructed display is covered with a copper plate, allowing each SMA actuator to be stably situated at the designed location with its height properly adjusted, as shown in Figure 4c. The height was adjusted by cutting the pin to a specific length of 19.2 mm. A user places the index finger on the copper plate, as shown in Figure 4d, and perceives the stimulus of vibration and temperature. While the thermal stimulation unit is driven, a fan situated below the circuit board is operated to generate an airflow to release the heat from the heatsinks.

The SMA actuators and thermal stimulation unit are driven by a specially designed current controller to provide sufficient electric current, by amplifying the control signal generated by the Raspberry Pi microcomputer. The motor driver also controls the current

to flow bi-directionally, allowing the thermal unit to work for both cooling and heating. These controlling circuits are implemented on the backside of the touch panel, making the whole system compact, as shown in Figure 5. An operator is able to simply generate the desired stimuli by setting the three control parameters presented on the interface panel, which are temperature, vibrating frequency, and duty ratio.

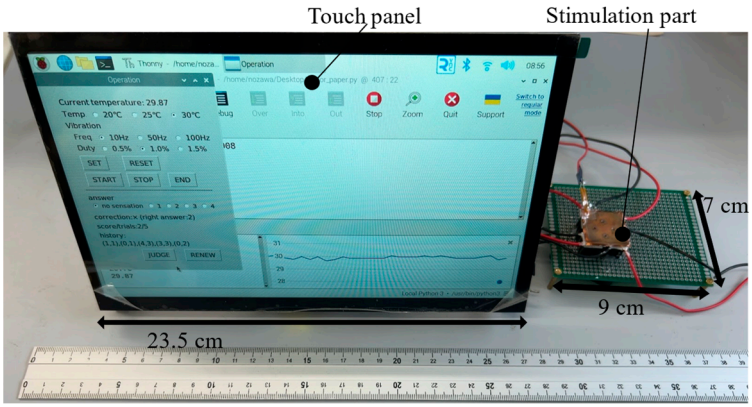

Figure 5. Overview of the total system.

3.4. Control Software and User Interface

We designed two different dialog boxes to provide user interfaces for controlling the tactile display, as shown in Figure 6, which are (a) a dialog box for custom parameter settings with a virtual keyboard and (b) a dialog box with preliminary defined parameter values. An operator selects one of the dialogues based on the preference. By using the interface (a), an operator is able to customize the driving conditions of the actuators for examining detailed tactile sensations. On the other hand, by using the interface (b), an operator is able to check the necessary tactile sensitivity by using the preliminary-selected parameter values for driving the device. In both the interfaces, the temperature of the display is presented at the top of the display and updated every 0.5 s.

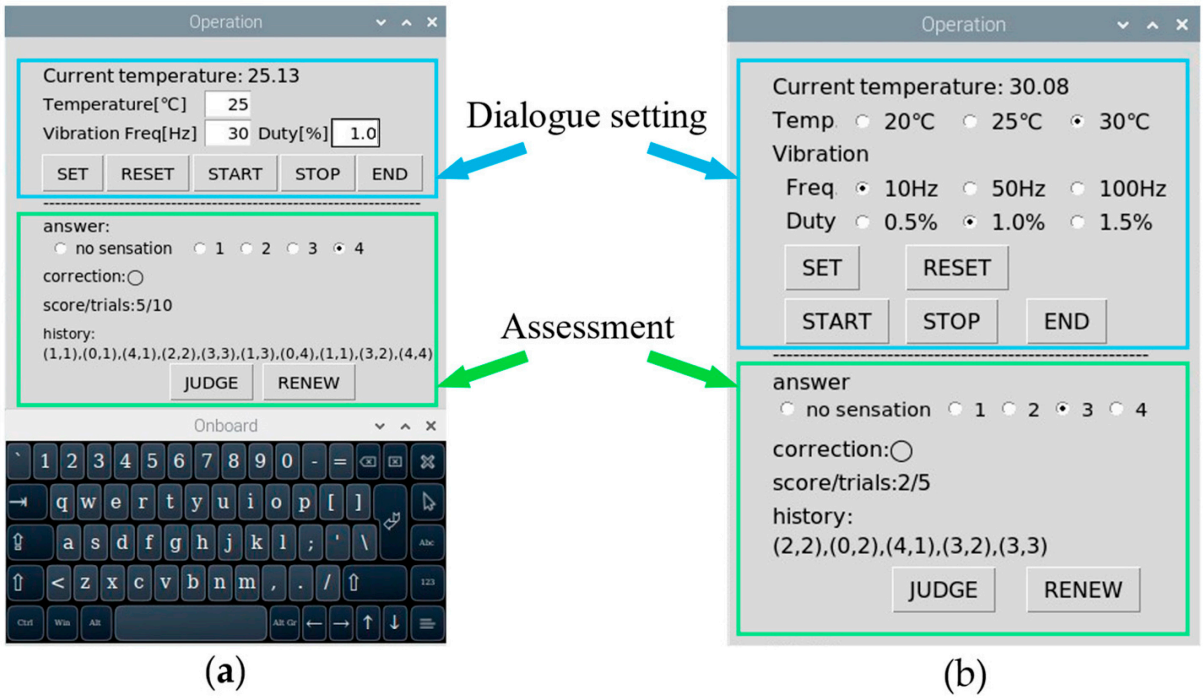

Figure 6. Two different user interfaces. (**a**) A dialog box with custom parameter settings and a virtual keyboard. (**b**) A dialog box with pre-defined parameter values.

4. Preliminary Experiment for Selecting Driving Parameters for Tactile Assessment

A preliminary experiment was conducted by employing one subject (a 24-year-old male) to determine the effective parameters for the assessment of cutaneous sensation. Various conditioned vibrations are generated by changing the pulse frequencies and the duty ratios, and in this experiment, we tested the frequencies of 5, 10, 50, 80, 100, and 150 Hz under the room temperature at 25 degrees, by considering the tactile perceptions related with the human mechanoreceptors RA I and RA II.

The qualitative results recognized by the subject were obtained as follows. At 5 and 10 Hz, he reported the sensations like being finely tapped. On the other hand, vibrations of other frequencies were perceived as small vibratory sensations with different tactile feelings. The temporal resolution of the human skin is reported to be approximately 30 to 80 ms [41]. By adopting the temporal resolution value of 30 ms, which presented the most sensitive sensation in the reference [41], the condition of the pulse current to provide vibratory sensation whose time interval is longer than the temporal resolution can be given by the following inequality.

$$\frac{100-d}{100f} > 30 \times 10^{-3} \tag{1}$$

By deforming this equation, we obtain

$$f < \frac{100-d}{3}. \tag{2}$$

Here, if we adopt the temporal resolution as 80 ms, the condition of pulse current is calculated as follows.

$$f < \frac{100-d}{8}. \tag{3}$$

The frequencies below 10 Hz satisfy these conditions; therefore, the vibrations below 10 Hz are perceived as discrete tapping stimuli, while the vibrations with frequencies above 50 Hz are recognized as continuous vibratory sensations, inducing different tactile feelings in accordance with vibration frequencies as illustrated in Figure 7.

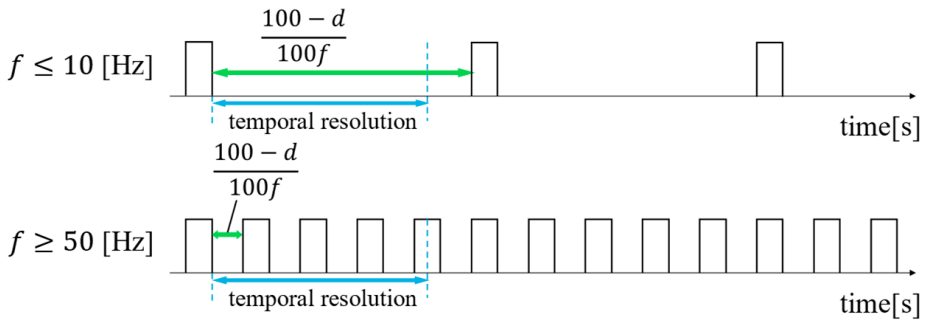

Figure 7. Relationship between the frequency and time resolution.

In addition, the subject reported the influence of the duty ratio. At 5 Hz, the vibrations were clearly recognized even when the duty ratio was considerably low. This implies that the frequency of 5 Hz is not appropriate for the assessment. At 10 Hz, the change in intensity was clearly recognized with the different duty ratios. In accordance with the increase in the duty ratio, the perceived sensation became greater. On the other hand, the difference in intensity was not distinct at 50 and 80 Hz within the duty ratio range of between 1.0 and 2.0%. At 100 and 150 Hz, like at 10 Hz, the perceived tactile sensation became greater at greater duty ratios. Vibrations at 150 Hz were not clearly recognized with the different duty ratios in comparison with the vibration of 100 Hz.

Based on the above experimental results, we decided to employ two frequencies, 10 and 100 Hz, for the cutaneous sensation assessment. The other conditions, including duty ratios and temperatures, will be described in the next chapter.

5. Experiment for the Assessment of the Cutaneous Sensations

We conducted a user experiment to investigate the temperature effects on tactile sensitivities related to the RA I and RA II receptors by presenting vibratory stimuli with different intensity levels by employing the novel tactile display.

Here, we selected six different vibrations in two temperature conditions, as shown in Table 1. The two temperatures were set at 20 and 30 degrees Celsius in the experiment. Thirty degrees Celsius is nearly the same as the average human fingertip temperature [42], while 20 degrees Celsius is in the response range of the cold receptors [43]. By considering the perception range against vibratory stimuli, the duty ratios were set to 0.5, 1.0, and 2.0% at 10 Hz. On the other hand, 1.5, 2.0, and 2.5% were employed at 100 Hz, in which the small duty ratio generates smaller vibration, and on the other hand, the great ratio presents greater physical stimuli. The displacement of the SMA actuators is the same under the same driving parameters.

Table 1. Three different duty ratios against two frequencies and two temperature conditions.

Temperature [°C] \ Frequency [Hz]	10		100	
20	0.5%	(Minimum)	1.5%	(Minimum)
	1.0%	(Medium)	2.0%	(Medium)
30	2.0%	(Maximum)	2.5%	(Maximum)

Nine subjects (7 males and 2 females, all right-handed) participated in the experiment. The number of subjects was determined by referring to the related works [5,6]. All subjects signed an informed consent after the experimental procedure was explained to them. A subject sat on a chair in front of the tactile display and was commonly instructed to place the tip of an index finger on the copper plate of the display to perceive the physical stimuli given by the tactile pins and the thermal unit. The same conditioned stimuli were presented to all the subjects, and we assessed the recognized sensations by the subjects. When the surface of the display reaches the target temperature within approximately 15 s, one of the SMA actuators is chosen randomly to present a vibratory stimulus. After 5 s from the beginning of touching, the subject answers which pin is vibrating through the interface dialog shown in Figure 6. Here, it is noted that the skin temperature was not measured in this experiment. Instead, we observed the display surface temperature and confirmed the temperature was kept stable while presenting the stimuli. At each condition, the stimulus presentation is repeated four times, which is equal to the number of pins in the display, and the number of correct answers is recorded as a score. This process is repeated for 12 conditions, and a quantitative assessment given by the scores ranging from 0 to 4 points is conducted.

6. Results and Discussion

The experimental results are summarized in Figure 8. The scores decreased at 20 degrees Celsius compared to 30 degrees Celsius. The tendency of lower sensitivity at a lower temperature is remarkable at 100 Hz. This is consistent with the previous reports, which reveal that cold stimulus worsens the sensitivity at higher frequencies. For a better understanding of the thermo-tactile interactions, the temperature dependence at higher frequencies and the influences of warmer stimuli will be further investigated by including detailed parameter conditions in our next work.

Regarding the duty ratios, the greater duty ratios resulted in higher scores, as we expected. At 10 Hz vibration, the average score at 2.0% duty ratio obtained 3.9 points, while the score at 0.5% was only 0.94 points. On the other hand, at 100 Hz vibration, the stimuli of all the duty ratios were well recognized, and there was a tendency for the greater duty ratios to obtain better recognition results. These results indicate that the greater duty ratios provide vibrations that are easier to perceive. We verify that the proposed tactile device is able to present different physical stimuli by controlling the pulse frequencies and the duty

ratios. On the other hand, at 100 Hz, the variation in the scores is comparatively greater than in the cases of 10 Hz presentations. The results suggest the difference in sensitivities among subjects against the stimuli with higher frequencies. Further considerations are left to our future work.

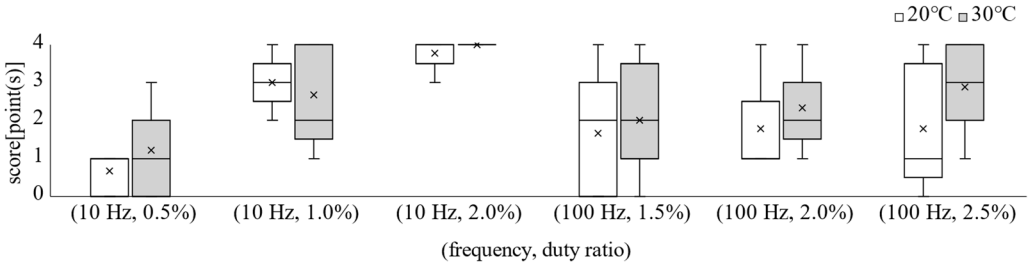

Figure 8. Boxplots of the scores under different conditions.

Figure 9 shows the change in recognition response by trial times at each condition. The blue markers represent the number of subjects who correctly recognized the vibration. The red markers show the number of subjects who answered a certain number but did not correctly identify the vibrating pin, while the green markers indicate the number of those who did not feel vibrations. The trial times did not have any particular effects on the response types. Therefore, it is estimated that adaptations, fatigue, and accustom by repeated trials did not occur in the use of our tactile device.

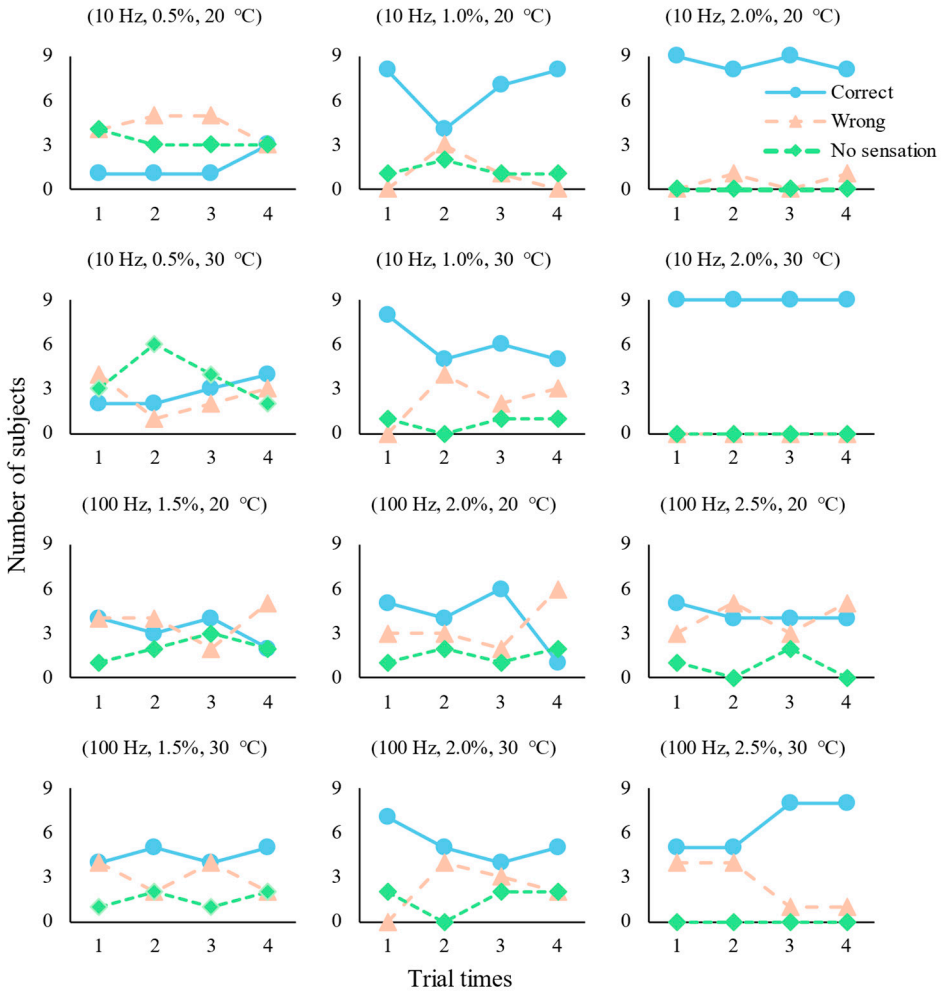

Figure 9. Change in recognition response by trial times.

Figure 10 presents the confusion matrices between the correct answers and the subject's answers in each condition. The vibrations at 10 Hz with a 0.5% duty ratio tended to be reported with no sensation. The vibrations at 100 Hz at 20 degrees Celsius were confused with other pins situated in adjacent locations, though the physical stimuli were recognized. The ratios of correctly identifying the vibrating pin tended to increase in accordance with the increase in the duty ratio at 10 Hz, while it was nearly stable at 100 Hz.

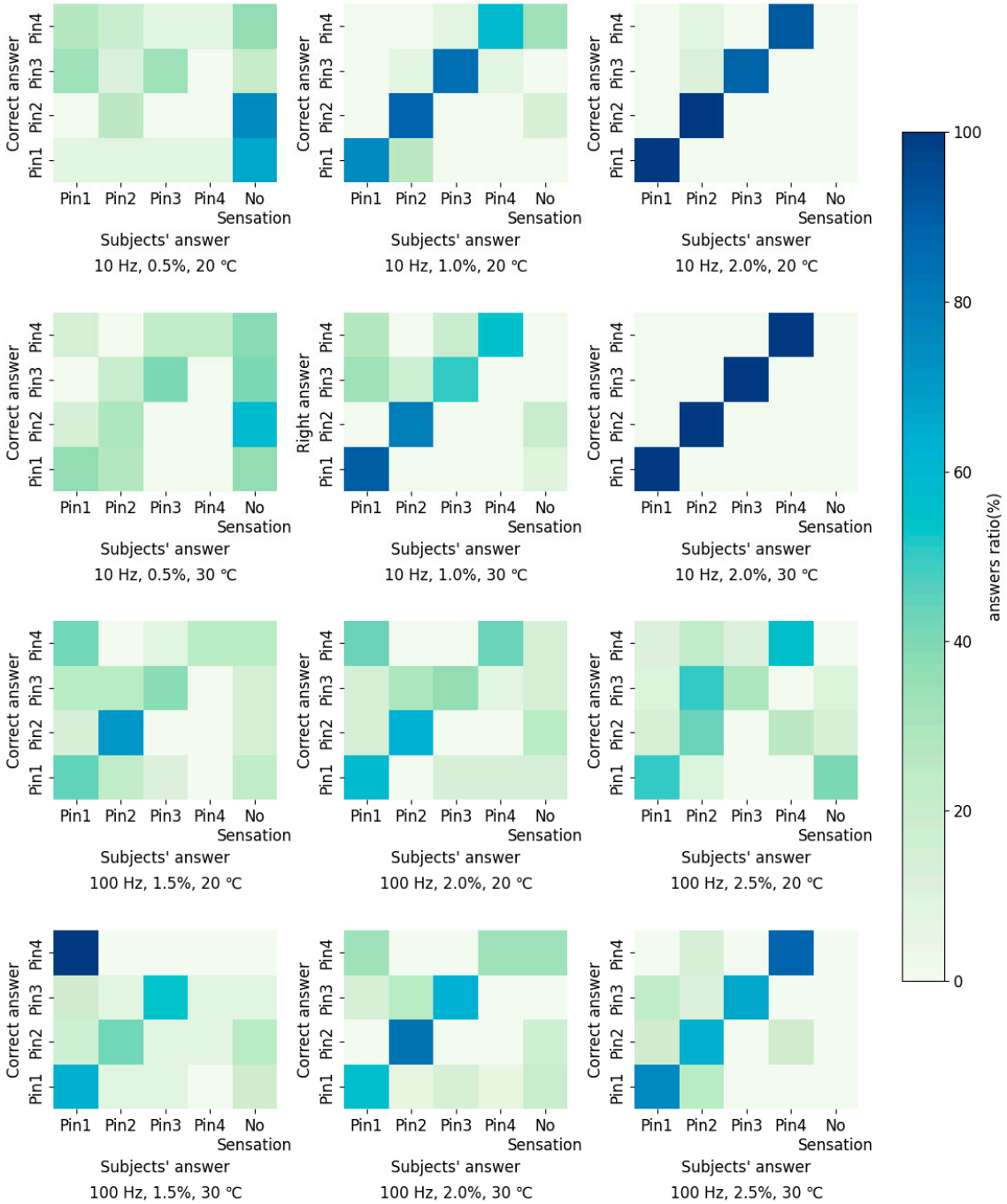

Figure 10. Confusion matrices between the correct answers and the subject's answers.

By using the proposed method, even if a subject does not identify a vibrating pin, he/she is able to give an answer randomly with a ratio of 25%. These problems would also be caused in the case of commonly used vision acuity tests using E chart [44]. In the next

study, we will increase the number of patterns for the selection to decrease the chance of random selection.

7. Conclusions

This paper introduced a novel tactile display for presenting vibrations and thermal stimuli simultaneously. The system consists of vibration actuators using SMA wires and a thermal stimulation unit based on Peltier elements. Various tactile patterns were generated by controlling three parameters, which are the frequency, duty ratio of vibration, and temperature. The user experiments were conducted to verify the performance of the developed device and also to investigate the thermal-tactile interaction. The results revealed that the different intensity levels of physical stimuli were successfully generated by controlling parameters, which suggested a possible employment for tactile diagnosis in the medical field.

In the future, we will further explore the tactile sensation in relation to the vibrotactile stimuli and the thermal stimuli by presenting much various and detailed tactile patterns, such as higher or lower frequency vibrations and different temperatures. Since our device installs four vibration pins and a thermal unit, which are independently driven and controlled, plural pins can be driven simultaneously or with time delays. This characteristic will introduce a novel user experiment to ask users to answer the vibrating patterns of pins or the vibrating order of pins, which will be used for the precise diagnosis of tactile sensation. In the next study, we will test our device for the diagnosis of subjects who have abnormal tactile sensation and lower tactile sensitivity. The system will introduce a new quantitative diagnosis of tactile sensation in the medical field.

Author Contributions: Conceptualization, T.N., R.L. and H.S.; methodology, T.N., R.L. and H.S.; software, T.N.; validation, T.N. and H.S.; formal analysis, T.N.; investigation, T.N.; resources, H.S.; data curation, T.N.; writing—original draft preparation, T.N.; writing—review and editing, R.L and H.S.; visualization, T.N.; supervision, H.S.; project administration, H.S.; funding acquisition, H.S. All authors have read and agreed to the published version of the manuscript.

Funding: This research was funded by JSPS KAKENHI Grant-in-Aid for Scientific Research (B) 20H04214.

Data Availability Statement: The original contributions presented in the study are included in the article.

Acknowledgments: We would like to thank the professors at Nippon Medical School for valuable discussions.

Conflicts of Interest: The authors declare no conflicts of interest.

References

1. Qiu, Y.; Lu, Z.; Pei, Q. Refreshable Tactile Display Based on a Bistable Electroactive Polymer and a Stretchable Serpentine Joule Heating Electrode. *ACS Appl. Mater. Interfaces* **2018**, *10*, 24807–24815. [CrossRef] [PubMed]
2. Trinitatova, D.; Tsetserukou, D. DeltaTouch: A 3D Haptic Display for Delivering Multimodal Tactile Stimuli at the Palm. In Proceedings of the 2019 IEEE World Haptics Conference (WHC), Tokyo, Japan, 9–12 July 2019; pp. 73–78.
3. Bau, O.; Poupyrev, I.; Israr, A.; Harrison, C. TeslaTouch: Electrovibration for Touch Surfaces. In Proceedings of the 23nd Annual ACM Symposium on User Interface Software and Technology, New York, NY, USA, 3–6 October 2010; Association for Computing Machinery: New York, NY, USA, 2010; pp. 283–292.
4. Rajaei, N.; Ohka, M.; Nomura, H.; Komura, H.; Matsushita, S.; Miyaoka, T. Tactile Mouse Generating Velvet Hand Illusion on Human Palm. *Int. J. Adv. Robot. Syst.* **2016**, *13*, 1729881416658170. [CrossRef]
5. Vardar, Y.; Güçlü, B.; Basdogan, C. Effect of Waveform on Tactile Perception by Electrovibration Displayed on Touch Screens. *IEEE Trans. Haptics* **2017**, *10*, 488–499. [CrossRef] [PubMed]
6. Alonzo, M.D.; Engels, L.F.; Controzzi, M.; Cipriani, C. Electro-Cutaneous Stimulation on the Palm Elicits Referred Sensations on Intact but Not on Amputated Digits. *J. Neural Eng.* **2017**, *15*, 016003. [CrossRef] [PubMed]
7. Matsunaga, T.; Totsu, K.; Esashi, M.; Haga, Y. Tactile Display Using Shape Memory Alloy Micro-Coil Actuator and Magnetic Latch Mechanism. *Displays* **2013**, *34*, 89–94. [CrossRef]
8. Guo, Y.; Tong, Q.; Zhao, P.; Zhang, Y.; Wang, D. Electromagnetic-Actuated Soft Tactile Device Using a Pull–Push Latch Structure. *IEEE Trans. Ind. Electron.* **2023**, *70*, 10344–10352. [CrossRef]

9. Luo, Y.; Sun, J.; Zeng, Q.; Zhang, X.; Tan, L.; Chen, A.; Guo, H.; Wang, X. Programmable Tactile Feedback System for Blindness Assistance Based on Triboelectric Nanogenerator and Self-Excited Electrostatic Actuator. *Nano Energy* **2023**, *111*, 108425. [CrossRef]
10. Banach, M.; Juranek, J.K.; Zygulska, A.L. Chemotherapy-induced Neuropathies—A Growing Problem for Patients and Health Care Providers. *Brain Behav.* **2016**, *7*, e00558. [CrossRef]
11. Motoo, Y.; Cameron, S. Significance of Kampo Medicine for Cancer Supportive Care: Overview. *Tradit. Kampo Med.* **2023**, *10*, 16–19. [CrossRef]
12. Liu, Q.; Ghodrat, S.; Huisman, G.; Jansen, K.M.B. Shape Memory Alloy Actuators for Haptic Wearables: A Review. *Mater. Des.* **2023**, *233*, 112264. [CrossRef]
13. Baba, Y.; Igarashi, H.; Liu, R.; Sawada, H. A Pin-Array Tactile Display Using Shape-Memory Alloy Wires for the Presentation of Various Tactile Sensation. *Int. J. Innov. Comput. Inf. Control.* **2024**, *20*, 653–664.
14. Chen, Y.; Shen, J.; Sawada, H. A Wearable Assistive System for the Visually Impaired Using Object Detection, Distance Measurement and Tactile Presentation. *Intell. Robot.* **2023**, *3*, 420–435. [CrossRef]
15. Oya, R.; Sawada, H. An SMA Transducer for Sensing Tactile Sensation Focusing on Stroking Motion. *Materials* **2023**, *16*, 1016. [CrossRef]
16. Chujo, T.; Sawada, H. The Application of Micro-Vibratory Phenomena of a Shape-Memory Alloy Wire to a Novel Vibrator. *Vibration* **2023**, *6*, 584–598. [CrossRef]
17. Liu, R.; Zheng, H.; Hliboký, M.; Endo, H.; Zhang, S.; Baba, Y.; Sawada, H. Anatomically-Inspired Robotic Finger with SMA Tendon Actuation for Enhanced Biomimetic Functionality. *Biomimetics* **2024**, *9*, 151. [CrossRef]
18. Fukuchi, H.; Sawada, H. An Inchworm Robot with Self-Healing Ability Using SMA Actuators. *J. Robot. Mechatron.* **2023**, *35*, 1615–1621. [CrossRef]
19. Dinulescu, S.; Tummala, N.; Reardon, G.; Dandu, B.; Goetz, D.; Topp, S.; Visell, Y. A Smart Bracelet Supporting Tactile Communication and Interaction. In Proceedings of the 2022 IEEE Haptics Symposium (HAPTICS), Santa Barbara, CA, USA, 21–24 March 2022; pp. 1–7.
20. Sundari, J.; Hamimah; Handayani, P.; Yunita; Lesmono, I.D.; Rahmayu, M.; Kusumawardhani, P.; Budiarti, Y.; Fadilah; Nurhayati. Expert System to Detect Human's Skin Diseases Using Forward Chaining Method Based On Web Mobile. *MATEC Web Conf.* **2018**, *218*, 02015. [CrossRef]
21. Johansson, R.S. Tactile Afferent Units with Small and Well Demarcated Receptive Fields in the Glabrous Skin Area of the Human Hand. In *Sensory Functions of the Skin of Humans*; Kenshalo, D.R., Ed.; Springer: Boston, MA, USA, 1979; pp. 129–152. ISBN 978-1-4613-3039-4.
22. Johnson, K.O. The Roles and Functions of Cutaneous Mechanoreceptors. *Curr. Opin. Neurobiol.* **2001**, *11*, 455–461. [CrossRef]
23. Maeno, T.; Kobayashi, K.; Yamazaki, N. Relationship between the Structure of Human Finger Tissue and the Location of Tactile Receptors. *JSME Int. J. Ser. C* **1998**, *41*, 94–100. [CrossRef]
24. Deflorio, D.; Di Luca, M.; Wing, A.M. Skin and Mechanoreceptor Contribution to Tactile Input for Perception: A Review of Simulation Models. *Front. Hum. Neurosci.* **2022**, *16*, 862344. [CrossRef]
25. Miyaoka, T.; Mano, T.; Fukuda, H. Threshold Curves and Equal-Sensation Contours for Low Frequency Vibrotactile Stimuli on the Human Glabrous Skin. *Jpn. Psychol. Res.* **1985**, *27*, 145–153. [CrossRef]
26. Green, B.G. The Effect of Skin Temperature on Vibrotactile Sensitivity. *Percept. Psychophys.* **1977**, *21*, 243–248. [CrossRef]
27. Zhang, Z.; Francisco, E.M.; Holden, J.K.; Dennis, R.G.; Tommerdahl, M. The Impact of Non-Noxious Heat on Tactile Information Processing. *Brain Res.* **2009**, *1302*, 97–105. [CrossRef]
28. Yang, G.-H.; Kyung, K.-U.; Srinivasan, M.A.; Kwon, D.-S. Quantitative Tactile Display Device with Pin-Array Type Tactile Feedback and Thermal Feedback. In Proceedings of the 2006 IEEE International Conference on Robotics and Automation, Orlando, FL, USA, 15–19 May 2006; pp. 3917–3922.
29. Singhal, A.; Jones, L.A. Perceptual Interactions in Thermo-Tactile Displays. In Proceedings of the 2017 IEEE World Haptics Conference (WHC), Munich, Germany, 6–9 June 2017; pp. 90–95.
30. Singhal, Y.; Wang, H.; Gil, H.; Kim, J.R. Mid-Air Thermo-Tactile Feedback Using Ultrasound Haptic Display. In Proceedings of the 27th ACM Symposium on Virtual Reality Software and Technology, Osaka, Japan, 8–10 December 2021; Association for Computing Machinery: New York, NY, USA, 2021; pp. 1–11.
31. Gallo, S.; Son, C.; Lee, H.J.; Bleuler, H.; Cho, I.-J. A Flexible Multimodal Tactile Display for Delivering Shape and Material Information. *Sens. Actuators Phys.* **2015**, *236*, 180–189. [CrossRef]
32. Gharat, S.S.; Shetty, Y.; McDaniel, T. A Vibrothermal Haptic Display for Socio-Emotional Communication. In Proceedings of the HCI International 2021—Late Breaking Papers: Multimodality, eXtended Reality, and Artificial Intelligence, Virtual Event, 24–29 July 2021; Stephanidis, C., Kurosu, M., Chen, J.Y.C., Fragomeni, G., Streitz, N., Konomi, S., Degen, H., Ntoa, S., Eds.; Springer International Publishing: Cham, Switzerland, 2021; pp. 17–30.
33. Oyama, Y.; Tokunaga, T.; Nagata, M.; Kazuhito, F. Development of Complex Inspection Device for Cutaneous Sense Diagnosis. In Proceedings of the Second International Conference on Innovative Computing, Informatio and Control (ICICIC 2007), Kumamoto, Japan, 5–7 September 2007; p. 134.
34. Kawasegi, N.; Fujii, M.; Shimizu, T.; Sekiguchi, N.; Sumioka, J.; Doi, Y. Evaluation of the Human Tactile Sense to Microtexturing on Plastic Molding Surfaces. *Precis. Eng.* **2013**, *37*, 433–442. [CrossRef]

35. D'Angelo, M.L.; Cannella, F.; Liberini, P.; Caldwell, D.G. Development and Validation of a Tactile Sensitivity Scale for Peripheral Neuropathy Screening. In Proceedings of the 2014 36th Annual International Conference of the IEEE Engineering in Medicine and Biology Society, Chicago, IL, USA, 26–30 August 2014; pp. 4823–4826.
36. Amin-Ahmadi, B.; Noebe, R.D.; Bucsek, A.N.; Steirer, K.X.; Stebner, A.P. The Atomic Structure and Mechanisms of Formation of Some Geometrically Incompatible Interfaces within Cubic B2 Austenite—Monoclinic B19′ Martensite Shape Memory Alloy Microstructures. *Mater. Charact.* **2023**, *204*, 113173. [CrossRef]
37. Gangil, N.; Siddiquee, A.N.; Maheshwari, S. Towards Applications, Processing and Advancements in Shape Memory Alloy and Its Composites. *J. Manuf. Process.* **2020**, *59*, 205–222. [CrossRef]
38. Sawada, H. Micro-Vibration Actuators Driven by Shape-Memory Alloy Wires and Its Application to Tactile Displays. In Proceedings of the 2017 International Symposium on Micro-NanoMechatronics and Human Science (MHS), Nagoya, Japan, 3–6 December 2017; pp. 1–5.
39. Shilpa, M.; Raheman, M.; Aabid, A.; Baig, M.; Veeresha, R.; Kudva, N. A Systematic Review of Thermoelectric Peltier Devices: Applications and Limitations. *Fluid Dyn. Mater. Process.* **2022**, *19*, 187–206. [CrossRef]
40. Manning, H.; Tremblay, F. Age Differences in Tactile Pattern Recognition at the Fingertip. *Somatosens. Mot. Res.* **2006**, *23*, 147–155. [CrossRef]
41. Yaguchi, A.; Atsumi, T.; Ide, M. Tactile Temporal Resolution. In *Encyclopedia of Autism Spectrum Disorders*; Volkmar, F.R., Ed.; Springer: New York, NY, USA, 2020; pp. 1–6. ISBN 978-1-4614-6435-8.
42. Kenshalo, D.R.; Holmes, C.E.; Wood, P.B. Warm and Cool Thresholds as a Function of Rate of Stimulus Temperature Change. *Percept. Psychophys.* **1968**, *3*, 81–84. [CrossRef]
43. Manasrah, A.; Crane, N.; Guldiken, R.; Reed, K.B. Perceived Cooling Using Asymmetrically-Applied Hot and Cold Stimuli. *IEEE Trans. Haptics* **2017**, *10*, 75–83. [CrossRef] [PubMed]
44. Sum, R.W.; Woo, G.C. Subjective Refractions Determined by Dyop® and LogMAR Chart as Fixation Targets. *Ann. Eye Sci.* **2022**, *7*, 34. [CrossRef]